ELSEVIER

Journal of Nuclear Materials 297 (2001) 279–284

journal of nuclear materials

www.elsevier.com/locate/jnucmat

Response of reduced activation ferritic steels to high-fluence ion-irradiation

H. Tanigawa [a,*], M. Ando [a], Y. Katoh [b], T. Hirose [c], H. Sakasegawa [c], S. Jitsukawa [a], A. Kohyama [b], T. Iwai [d]

[a] *Japan Atomic Energy Research Institute, Tokai, Naka, Ibaragi 319-1195, Japan*

[b] *Institute of Advanced Energy, Kyoto University, Gokasho, Uji, Kyoto 611-0011, Japan*

[c] *Graduate School of Energy Science, Kyoto University, Yosida honmachi, Sakyo, Kyoto 606-8501, Japan*

[d] *Research Associate, Research Center for Nuclear Science and Technology, The University of Tokyo, 2-22 Shirakata-Shirane, Tokai, Naka, Ibaragi 319-11, Japan*

Received 23 October 2000; accepted 27 May 2001

Abstract

Effects of high-fluence irradiation in fusion-relevant helium production condition on defect cluster formation and swelling of reduced activation ferritic/martensitic steels (RAFs), JLF-1 (Fe–9Cr–2W–V–Ta) and F82H (Fe–8Cr–2W–V–Ta), have been investigated. Dual-ion (nickel plus helium ions) irradiation using electrostatic accelerators was adopted to simulate fusion neutron environment. The irradiation has been carried out up to a damage level of 100 displacement per atom (dpa) at around 723 K, at the HIT facility in the University of Tokyo. Thin foils for transmission electron microscopy (TEM) were prepared with a focused ion beam (FIB) microsampling system. The system enabled not only the broad cross-sectional TEM observation, but also the detailed study of irradiated microstructure, since unfavorable effects of ferromagnetism of a ferritic steel specimen were completely suppressed with this system by sampling a small volume in interests from the irradiated material. © 2001 Elsevier Science B.V. All rights reserved.

PACS: 61.80.−x; 61.80.Jh; 28.52.F; 61.16.B

1. Introduction

Reduced activation ferritic/martensitic steels (RAFs) are leading candidates for the blanket/first wall structures of fusion demonstration power devices, mainly due to their neutron-irradiation-resistance, acceptable induced-radioactivity levels and maturity as industrial materials [1]. High energy neutrons from deuterium–tritium (D–T) plasma generated in such devices introduce displacement damage in alloys to form self-interstitials and vacancies, and also produce helium and hydrogen atoms through transmutational reactions. These radiation-produced point defects often cause void swelling, creep during irradiation and reduction of fracture toughness through microstructural changes [2,3]. It has been demonstrated for austenitic alloys that the ratio of generation rates between helium atoms and displacement damage (He/dpa ratio) strongly affects these irradiation-induced phenomena. It is hence necessary to carry out irradiation experiments with a typical He/dpa ratio for fusion neutron environment of about 10 atomic ppm (appm) He/dpa, in order to clarify the effect of irradiation on microstructural changes in fusion reactors [4].

The objective of this study is to simulate and understand the effect of irradiation on microstructures in (RAFs) to a high damage level with a He/dpa ratio mentioned above, utilizing a dual ion irradiation technique. The damage microstructure was analyzed in view of the effect of boundaries between grains and laths. The

---

[*] Corresponding author. Tel.: +81-29 282 6551; fax: +81-29 282 5922.

E-mail address: tanigawa@popsvr.tokai.jaeri.go.jp (H. Tanigawa).

PII: S 0 0 2 2 - 3 1 1 5 (0 1) 0 0 6 3 3 - X

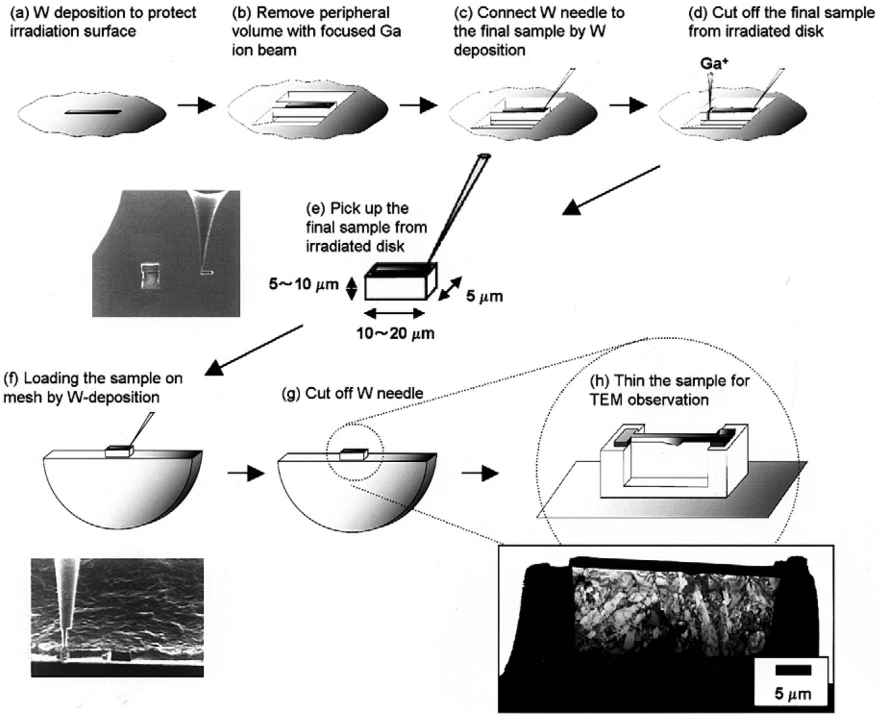

Fig. 1. Schematic drawing of sample processing procedure.

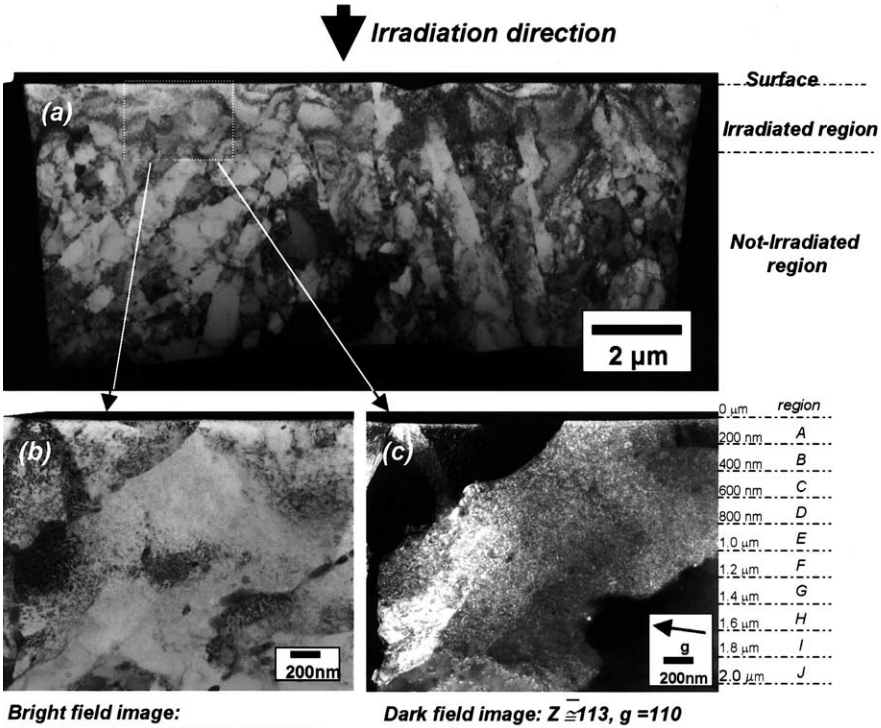

Fig. 2. Defects formed during irradiation to 100 dpa in F82H: (a) A TEM image of the thin foil specimen prepared with FIB processor. A depression by an indenter for hardness measurement is also shown. (b) A bright field image and (c) a dark field image of the area analyzed.

depth distribution of the microstructure was obtained for the analysis, because the damage distribution caused by ion irradiation varies with depth from the ion incident surface. For this purpose thin foil samples with sizes of about $20 \times 10 \times 0.05$ μm^3 were prepared along the beam direction using a focused ion beam (FIB) microprocessor with a microsampling apparatus. Procedures to obtain these foils are described in detail.

2. Experimental procedure

RAFs of JLF-1 (9Cr-2W-V-Ta) and F82H (8Cr-2W-V-Ta) were used for this experiment. Chemical compositions and heat mechanical treatments have been shown elsewhere [1,5]. The 3 mm diameter disks were used for irradiation. They were punched out from sheet materials, mechanically polished by the following series: SiC paper up to #4000, 9 and 3 μm diamond powder, 0.3 and 0.05 μm alumina powder, and completed by an electrolytic surface finish.

Ion irradiation was conducted at HIT facility operated by the University of Tokyo [4]. Ions of 4 MeV Ni^{3+} and 1 MeV He^{+} were chosen. Helium injection ratio to dpa (He/dpa) was set to 10 appm He/dpa at the depth between 500–700 nm from the incident surface with an energy degrader. Nominal displacement damage levels at the middle of dual irradiation range were 60 dpa for JLF-1 and 100 dpa for F82H. The irradiation temperature was controlled to be 723 K, as the maximum swelling was observed at nearly the same temperature, 703 K, in neutron-irradiated martensitic steels in the FFTF/MOTA [6]. The displacement damage rates were 1.5×10^{-3} dpa/s for 60 dpa irradiation and 3×10^{-3} dpa/s for 100 dpa irradiation, respectively.

Procedures to prepare thin foils for TEM observation are shown in Fig. 1; (a) W deposition (to reduce damage at the time of specimen fabrication in the region for observation), (b) removal of material with a fine Ga ion beam to obtain a foil, (c) welding of a W needle to the foil by W deposition, (d) cutting to separate the foil from the irradiated disk, (e) welding the foil to a mesh by W deposition and (f) electropolishing to remove a damaged layer near the foil surface formed during FIB processing. The last process is quite important for precise TEM observation. Electropolishing for a short period (for tens of milliseconds) was decided to be preferable for this process. An FIB processor (Hitachi FB-2000A) equipped with a microsampling system was used for ion machining and specimen manipulation. By this procedure, it became possible not only to get excellent cross-sectional TEM thin foils but also to decrease the processing time and the adverse effect of ferromagnetism of ferritic steel samples on TEM observation.

Microstructural inspections were performed using HITACHI HF-2000 and JEOL JEM-2000FX, and microchemical analysis was performed using an EDX system (Noran Voyager-2000) equipped to HF-2000. The thickness of the thin foils was determined by observing their secondary electron images under the FIB processor, which has a resolution about 10 nm.

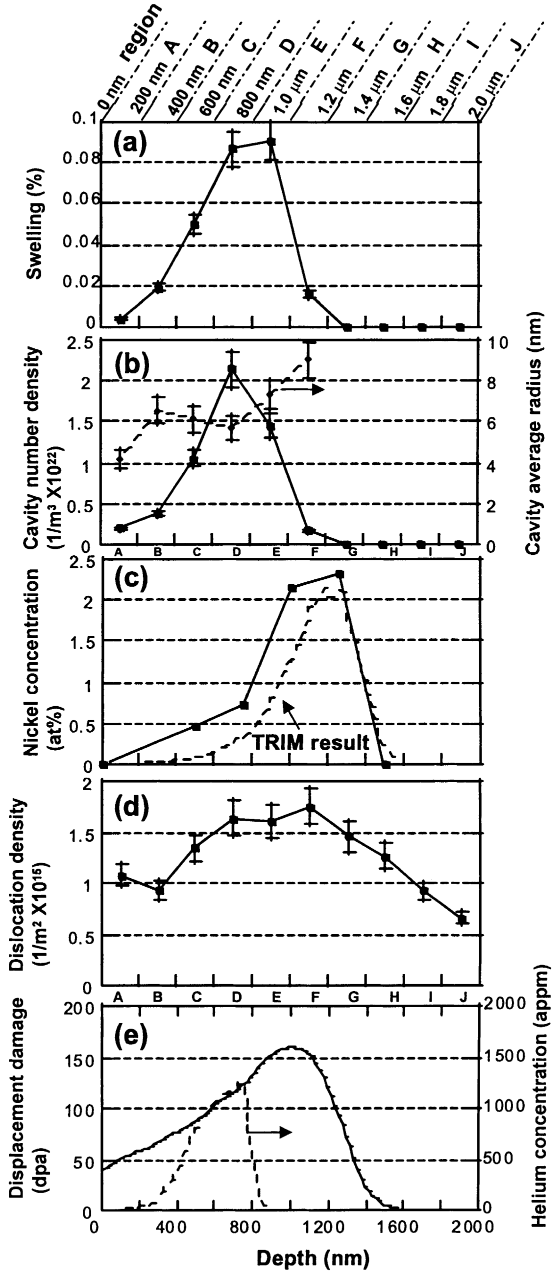

Fig. 3. The depth dependence of: (a) swelling; (b) cavity number density and average radius; (c) nickel concentration with calculated result; (d) dislocation density; (e) damage and helium concentration calculated with TRIM92.

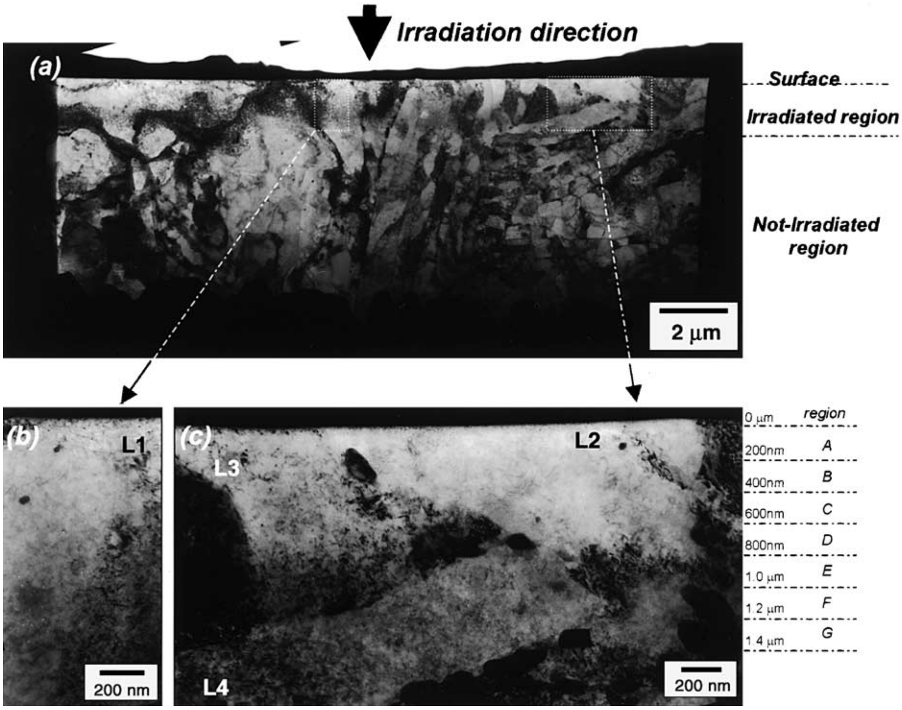

Fig. 4. TEM images of the thin foil prepared from JLF-1 specimen irradiated to 60 dpa at 723 K: (a) Four laths of L1, L2, L3 and L4 are seen; (b) Cavities in L1; (c) Cavities in L2, L3 and L4. Swelling and cavity number density in L4 were higher than those in other laths at the same depths from the incident surface.

3. Results and discussion

3.1. F82H irradiated up to 100 dpa

A large number of defects were formed in the region with the depth less than 1.5 μm from the incident surface during irradiation, as seen in Fig. 2(a). The depth distributions of the cavities and dislocations from the incident surface are summarized in Fig. 3, together with that of injected nickel atoms. Distributions of the clusters were affected by lath boundaries and prior-austenite grain boundaries. To avoid the effect of such boundaries, the analysis was conducted in a single lath extending from the incident surface to a depth of 2 μm (see a lath in the box in Fig. 2(a)). Analyses for cavities and dislocations have been done with bright field and dark field images, respectively. These images are shown in Figs. 2(b) and (c). The effect of the boundaries on the distributions will be discussed in the following section.

The distribution of dislocations agreed well with that of dpa obtained with TRIM code. The cavity number density peaked in D region in Figs. 2 and 3, where most of the helium atoms were injected. Swelling attained maximal in the regions of D and E. The concentration profile of injected nickel estimated by EDX slightly shifted toward the incident surface in comparison with TRIM result. The nickel level in regions D and E was measured to be about 0.6 at.%. In the regions of E and F, while the levels of displacement damage were almost the same, swelling levels were markedly different. Smaller injected helium level or higher nickel level might result in the smaller swelling in region F. Here, nickel is expected to increase sink strength and consequently to reduce swelling, through the enhancement of carbide precipitation formerly reported for the same steel [7]. Concerning the effect of He/dpa on cavity formation, present results qualitatively agreed with the previous observation [2] that lower He/dpa caused lower number density but larger size of cavities.

3.2. JLF-1 irradiated up to 60 dpa

Fig. 4 shows TEM images of a thin foil prepared from JLF-1 irradiated to 60 dpa. To examine the effect of lath boundaries on the distribution of cavities, four laths labeled L1, L2, L3 and L4 were selected and the distributions in the laths were compared. L1 extended from the incident surface to a depth of 4 μm. L2 and L3 extended to a depth of about 1 μm. L4 ranged from the depth of 1 to 2 μm.

Depth dependence of the swelling, cavity number density and cavity average radius in the laths are summarized in Fig. 5. Swelling and the number density of cavities at depths ranging roughly from 0.7 to 1 μm in the lath L4 were more than twice as large as those found in the other laths. Because the average radius of cavities in lath L4 was in the similar range of those in the other laths, the larger swelling of this lath was mainly due to the higher number density.

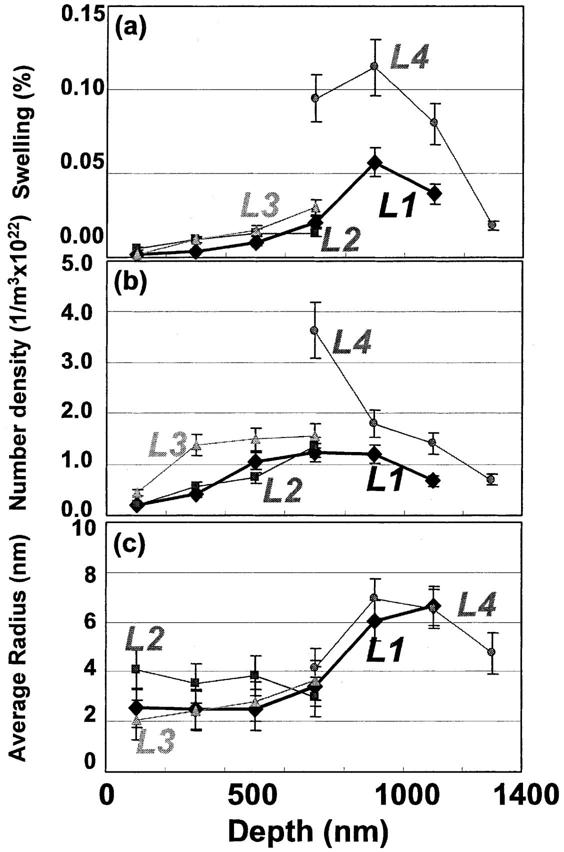

Fig. 5. The depth dependence of (a) swelling, (b) cavity number density and (c) cavity average radius in different laths.

The other research of ion irradiation documented that gas atoms like helium should be needed for the nucleation of cavities in commercial and complex martensitic alloys [2]. Therefore, the presence of cavities close to the surface (regions A and B) in laths L1, L2 and L3 may reflect substantial motion of implanted helium atoms toward the surface, since, in this experiment, most of them were deposited at the depth ranging from 500 to 700 nm. In parallel with this, the high number density of cavities in lath L4 in the region with the depth from 0.6 to 1 μm (region D, E) might be caused as the injected helium atoms in lath L4 would be prevented to escape from the incident surface. This larger cavity population arisen in lath L4 could also be explained in terms of sink strength as follows. The lath boundary seems to have worked as a point defect sink, because there was a tendency that large cavities were not observed near the lath boundary as shown in Fig. 6. Having a common with this, the free surface is expected to exhibit similar behavior but in a more pronounced manner. The vacancy concentration would thereby become higher in lath L4 relative to the other laths (L1, L2 and L3) and, as a consequence, cavity nucleation was presumably enhanced in the former lath. To confirm these analogy, further analysis are necessary to be done, and will be done in near future.

3.3. Important experimental factors for qualified high-fluence ion-irradiation experiments

From the observation on high quality cross-sectional TEM thin foils, it was indicated that effects of free

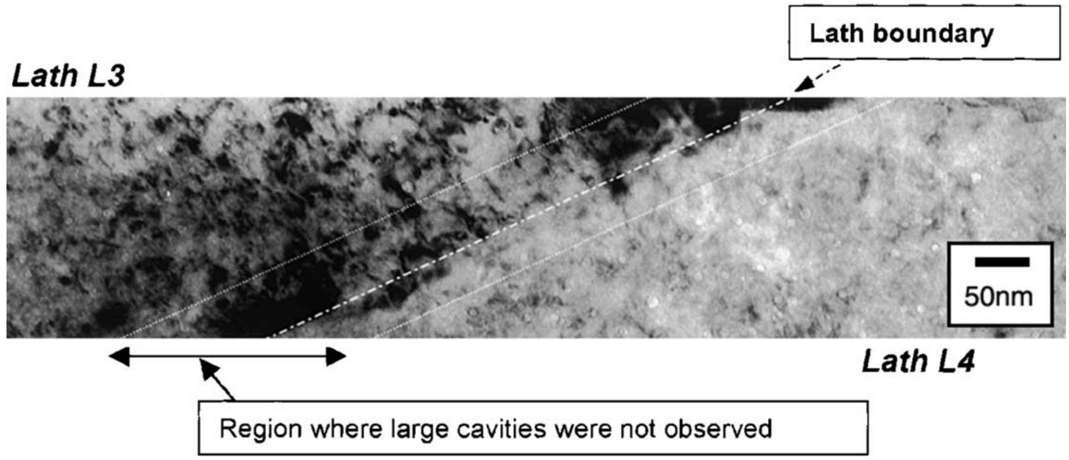

Fig. 6. Cavity distribution in vicinity of lath boundary between L3 and L4 in region from 600 to 800 nm in depth.

surface, lath boundary and injected atoms should be very strong, and those effects were enhanced by high-flux irradiation and high temperature. Through these facts, the experimental factors which are important for qualified high-fluence ion irradiation come to be clear as follows:

1. Self-ion irradiation is preferred to avoid the chemical effect of injected atoms.
2. Higher acceleration energy is preferred to obtain broad and flat damage profile in order to minimize the effect of the free surface.
3. Several laths should be analyzed to ensure the statistical accuracy of experimental data, because lath geometry could strongly affect the microstructure evolution.

4. Summary

To study the influence of high-fluence irradiation in fusion-relevant helium production condition on microstructure and swelling, cross-sectional TEM observation of dual ion irradiated F82H and JLF-1 were performed up to high doses with special concerns for the depth distribution of damaged microstructure.

1. Procedure of making high-quality cross-sectional TEM thin foils, utilizing FIB processor with a micro-sampling system, was presented.
2. In F82H irradiated up to 100 dpa, swelling of about 0.1% was observed, and the effect of injected nickel on swelling behavior was discussed.
3. In JLF-1 irradiated up to 60 dpa, different swelling behavior was observed among different martensite laths. The effects of free surface and lath boundary as sinks were discussed.
4. Important experimental factors for qualified high-fluence ion-irradiation experiments were proposed.

References

[1] A. Kohyama, Y. Kohno, K. Asakura, H. Kayano, J. Nucl. Mater. 212–215 (1994) 684.

[2] S. Hiwatashi, Y. Kohno, K. Asakura, A. Kohyama, J. Nucl. Mater. 179–181 (1991) 709.

[3] K. Shiba, I. Ioka, J.P. Robertson, M. Suzuki, A. Hishinuma, Euromat-96 (1996) 265.

[4] K. Asano, Y. Hosono, Y. Kohno, A. Kohyama, Nucl. Instrum. and Meth. B 17 (1986) 186.

[5] K. Shiba, M. Suzuki, A. Hishinuma, J. Nucl. Mater. 233–237 (1996) 309.

[6] T. Morimura, A. Kimura, H. Matsui, J. Nucl. Mater. 239 (1996) 118.

[7] E. Wakai, N. Hashimoto, K. Shiba, Y. Miwa, J.P. Robertson, R.L. Klueh, Fusion Reactor Materials DOE/ER-0313/25, 1999.